SCIENTIFIC REPORTS

OPEN

SUBJECT AREAS:
ELECTRON TRANSFER
POLYMER SYNTHESIS
ENZYME-CATALYSED REACTIONS
ATMOSPHERIC CHEMISTRY

Received
20 June 2013

Accepted
2 December 2013

Published
6 January 2014

Correspondence and requests for materials should be addressed to S.F.W. (wangsf@gxu.edu.cn) or G.Z.N. (gz.nonginguilin@163.com)

Artificial photosynthesis of oxalate and oxalate-based polymer by a photovoltaic reactor

Guangzai Nong[1], Shan Chen[1], Yuanjin Xu[3], Lijie Huang[1], Qingsong Zou[1], Shiqiang Li[2], Haitao Mo[1], Pingchuan Zhu[3], Weijian Cen[3] & Shuangfei Wang[2]

[1]Center for Sugar Engineering and Technology Research, Guangxi University, Nanning, Guangxi, 530004, P. R. China, [2]Institute of Light Industry and Food Engineering, Guangxi University, Nanning, Guangxi, 530004, P. R. China, [3]State key laboratory for conservation and utilization of subtropical agro-bioresources, Guangxi University, Nanning, Guangxi, 530004, P. R. China.

A photovoltaic reactor was designed for artificial photosynthesis, based on the reactions involved in high energy hydrogen atoms, which were produced from water electrolysis. Water and CO_2, under the conditions studied, were converted to oxalate ($H_2C_2O_4$) and a polymer. This was the first time that the oxalates and oxalate-based polymer were produced from the artificial photosynthesis process.

Getting inspirations from photosynthesis, people try to convert sunlight, water and carbon dioxide into carbohydrates and oxygen, and try to capture and store the solar energy in the other chemical bonds of a fuel by artificial means, which commonly is called artificial photosynthesis[1,2]. Having a great potential to reduce the CO_2 levels in Earth's atmosphere, and even produce fuel and food for anthropogenic activities, artificial photosynthesis has become a research hotspot[3–5]. So far, a variety of investigations on artificial photosynthesis have been carried out, including biomimetic approach[6,7], photocatalytic water splitting[1,8] and photocatalytic CO_2 reduction[2,9].

F. Kurayama, et al.[8,10] (2004) carried out an experiment on photo catalytic CO_2 reduction, getting HCOOH of 1.5–2.0 mmol/L. O. Ozcan, et al.[11] (2007) carried out experiments on water splitting combined CO_2 reduction, getting CH_3OH of 12–40 μmol/(g.catalyst). K Iizuka, et al.[12] (2011) carried out experiments on water splitting combined CO_2 reduction, getting H_2 of 10 mmol/h, CO of 4.3 mmol/h, and HCOOH 0.3 mmol/h. W. Lee, et al.[8] (2013) carried out an experiments on water splitting combined CO_2 reduction, getting H_2 of 124 nmol/h and CH_3OH of 522 nmol/h.

Although such artificial photosynthesizes successfully produced H_2, CO, HCOOH and CH_3OH, their efficiencies were still low and it did not yet produce sugar and polymer. Aim to produce sugar and other carbohydrates; a photovoltaic reactor for artificial photosynthesis was designed, based on the reaction involved in high energy hydrogen atoms. But it was far from our expectation; repeated several times, oxalate and oxalate-basic polymer were produced, instead of sugar and other carbohydrates. This was the first time that the oxalate and oxalate-based polymer were produced from the artificial photosynthesis process.

Results

The photovoltaic reactor for artificial photosynthesis was designed as Fig. 1.

The photovoltaic reactor consisted of a solar panel, an accumulator and an electrolytic cell. The solar panels were used to absorb solar energy, which was then converted into electric energy. The electrolytic cell was the sites of reactions, where the high energy hydrogen atoms and oxygen were produced by electrolysis of water. Then oxalate and polymer were subsequently synthesized.

The reactor was operated under the conditions studied for 480 hours, thereby a produced solution were obtained. Then the solution was analyzed by high performance liquid chromatography (HPLC) (Fig. 2), in which results showed the oxalate concentration was 17.32 g/L. For the 600 ml solution, total of 10.39 g of oxalate was obtained. The produced solution was treated in the following order: 1) strong acidic cation-exchange resin, 2) strong basic anion-exchange resin to remove the generated oxalate and other electrolytic compounds, and finally a neutral solution was obtained. The neutral solution thus obtained was concentrated and dried, yielding 0.76 g

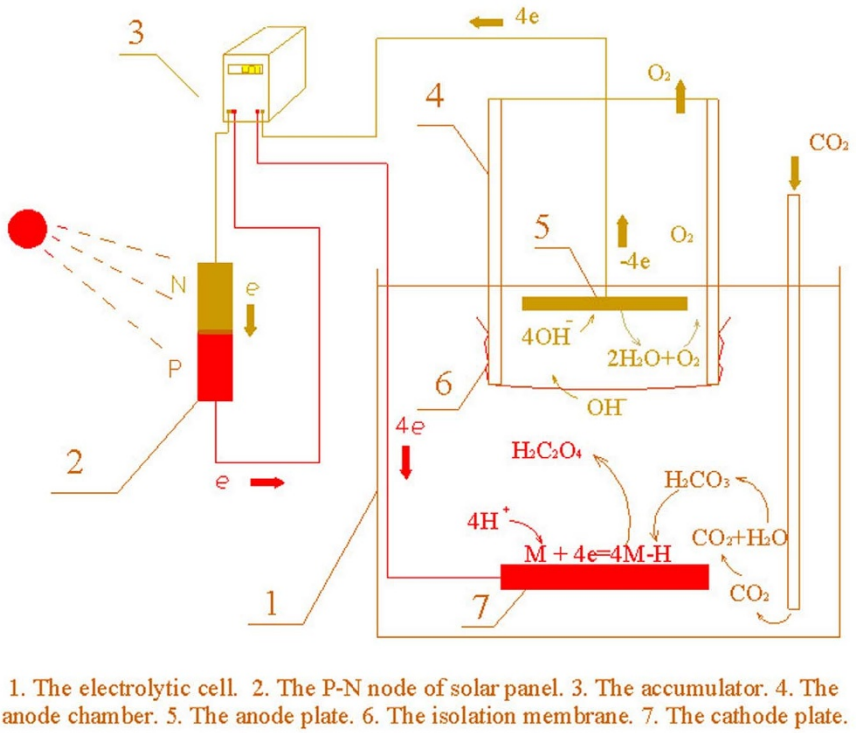

Figure 1 | **The photovoltaic reactor.** The photovoltaic reactor consists of a solar panel, an accumulator and an electrolytic cell. Which electrolytic cell consists of an anode chamber, an anode plate and cathode plate. And a 2.5 μm micro porous membrane of PTFE was used as the separation membrane.

neutral solid product, which was a transparent or translucent solid, shown in the supplementary figure 1 (S. Fig. 1).

The neutral solid product was analyzed by a gel permeation chromatography (GPC). The GPC spectrum contains two distinct peaks at 11.92 and 19.04 min, which accounted for 86.6% and 13.4%, respectively of the total peak area (S. Fig. 2). Based on the molecular weight calibration from globular proteins, the weight-average molecular weight (Mw) of the product at 11.92 min was 2.37×10^5 g/mol (Mw). The average molecular weight for the product at 19.04 min was 191.56 g/mol (S. Fig. 3 and 4). Therefore, the neutral solid product was regarded as a polymer.

To evaluate the performance efficiency of the reactor, the current efficiency, the electronic energy consumption efficiency and the cathode plate area efficiency were investigated. The current efficiency (E_i) is the ratio of the actual mass of special product (M_i) to the theoretical mass (M_{th}) of that product liberated according to Faraday's law, %; expressed as equation (1). The electronic energy consumption efficiency (E_{EEC}) is the actual mass of special products (M_i) divided by the electronic energy consumption (EEC), g/kwh; expressed as equation (2). The cathode plate area efficiency of (E_{CPA}) is the actual mass of special products (M_i) divided by the area of cathode plate (CPA) and time (t), g/(m^2. h); expressed as equation (3).

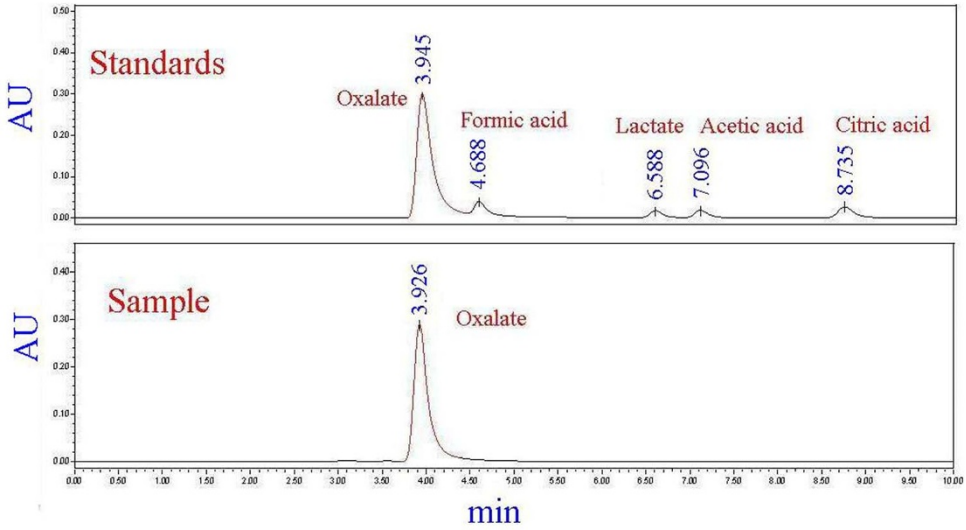

Figure 2 | **The HPLC spectrums for the produced solution.** It is the HPLC spectrum of the produced polymer, in which results show the oxalate absorption peak.

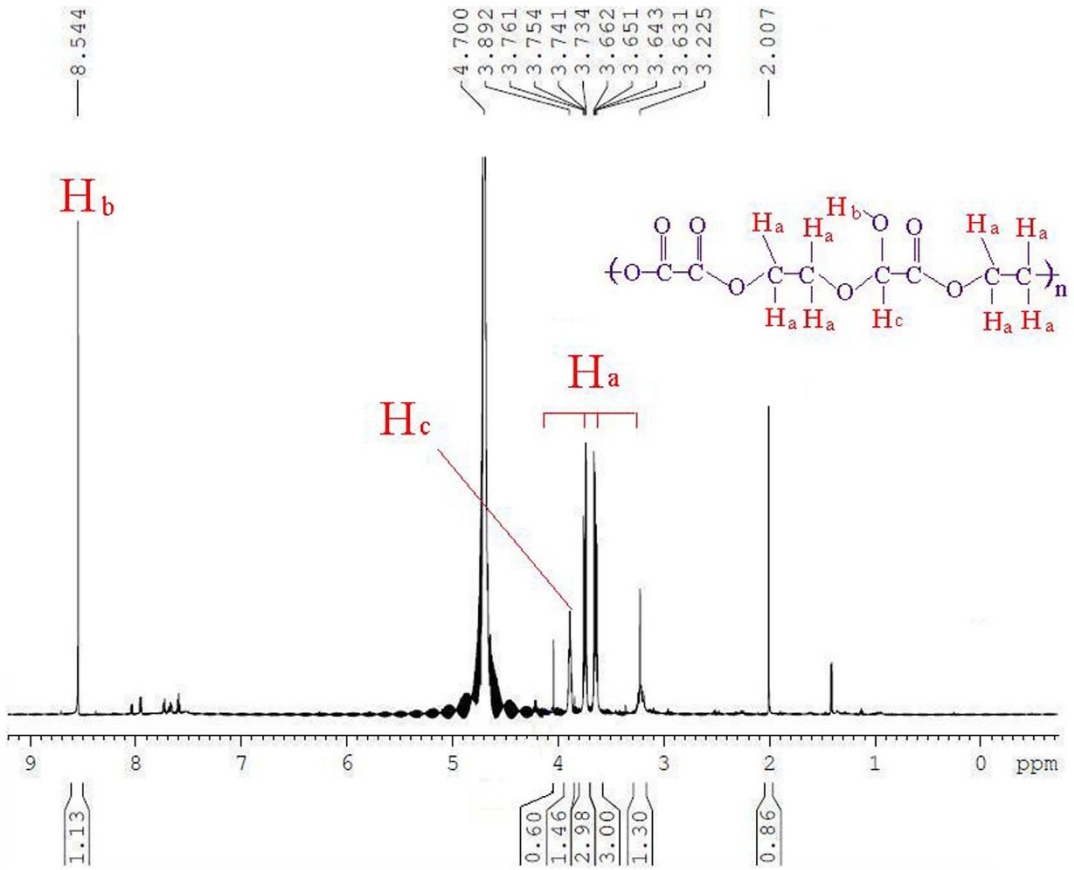

Figure 3 | The ^{1}H NMR results of the polymer. It is the ^{1}H NMR spectrum of the polymer. The proposed chemical structure of the polymer is attached in.

$$E_i = M_i/M_{th} \quad (1)$$

$$E_{EEC} = M_i/EEC \quad (2)$$

$$E_{CPA} = M_i/(CPA \times t) \quad (3)$$

Under the conditions studied, the current efficiency of the reactor was about 18.4% for oxalate and 5.18% for the polymer. The electronic energy consumption efficiency was 123.69 g/kwh for oxalate and 9.05 g/kwh for the polymer. The cathode plate area efficiency was 17.32 g/(m^2. h) for oxalate and 1.27 g/(m^2. h) for the polymer.

The elemental composition of the polymer is (wt%): 40.90% as carbon, 54.53% as oxygen and 4.55% as hydrogen. So, the formula of polymer is expressed as $C_8H_{10.7}O_8$. Based on the NMR results, the proposed structure of the polymer was given in Fig. 3. The polymer is made of oxalate, glycol and α-hydroxyl acetic acid.

Shown in Fig. 3, except the peak of solvent (D_2O, δ 4.70), there are three different hydrogen atoms in the ^{1}H NMR spectrum. Those four peaks at δ 3.225, 3.635, 3.745 and 4.035, noted as H_a, connected with C atoms at δ 62.29, may be assigned to CH_2 groups (S. Fig. 5 and 6)[13–16]. The peak at δ 8.544, noted as H_b, not connected with any C atoms (S. Fig. 6), but in the range of active H, is assigned to OH group[13,16,17]. The peak at δ 3.892, noted as H_c, connected with C atoms at δ 71.80, is assigned to CH group (S. Fig. 5 and 6)[16]. The peak at δ 2.007, not connected with any C atoms, and out of the range of active H (S. Fig. 6), can be regarded as an interference peak.

Shown in Fig. 4, there are four different C atoms in the ^{13}C NMR spectrum. Those at δ 171.13–171.16, noted as C_a, not connected with any H atoms (S. Fig. 6), may be assigned to C_2O_4 group[15,16,18]. The peak at δ 62.29, noted as C_b, connected with H atoms δ 3.225–4.035, is assigned to CH_2 group (S. Fig. 5 and 6)[16,19]. The peak at δ 71.80, noted as C_c, connected with H atoms of δ 3.892, is assigned to CH group (S. Fig. 5 and 6)[16,19,20]. The peak at δ 164.09, noted as C_d, not connected with any H atoms (S. Fig. 6), may be assigned to COO group[16,20,21].

The proposed structure of the polymer was further confirmed by Fourier transform infrared spectrometer (FTIR) and mass spectrometry (MS) results. There are five characteristic peaks in the FTIR spectrum. They are assigned to O-H[16,22–24], C=O[22,23,25,27], C-O[23,24], and H-C-H[23,24,26] (Fig. 5). These functional groups are consistent with the proposed polymer structure. Shown in Fig. 6 are the MS results, there are eight fragments that were less than 438 m/z, and all of them can be found in the proposed polymer structure.

Discussion

The reaction mechanisms are explained as follows: The high energy hydrogen atoms produced by water electrolysis are attached on the surface of the cathode plate; provisionally are presented in the form of M-H. Subsequently, reaction between M-H and M-H (or H_3O^+) takes place, producing hydrogen[28].

$$H^+ + M + e^- \rightarrow M\text{-}H + H_2O \quad (4)(\text{Volmer})$$

$$M\text{-}H + M\text{-}H \rightarrow 2M + H_2 \quad (5)(\text{Tafel})$$

$$M\text{-}H + H_3O^+ \rightarrow M + H_2 + H_2O \quad (6)(\text{Heyrovsky})$$

The reaction ability of the high energy hydrogen atom is strong because of the high energy level, which Gibbs free energy (ΔG) is −206.5 kJ/mol at the statute of temperature of 298 K, atmosphere. Therefore, when other substrates touch the cathode plate, reactions between substrate and the high energy hydrogen atoms should take place; produce new hydrogenated products, as described in Equation (7).

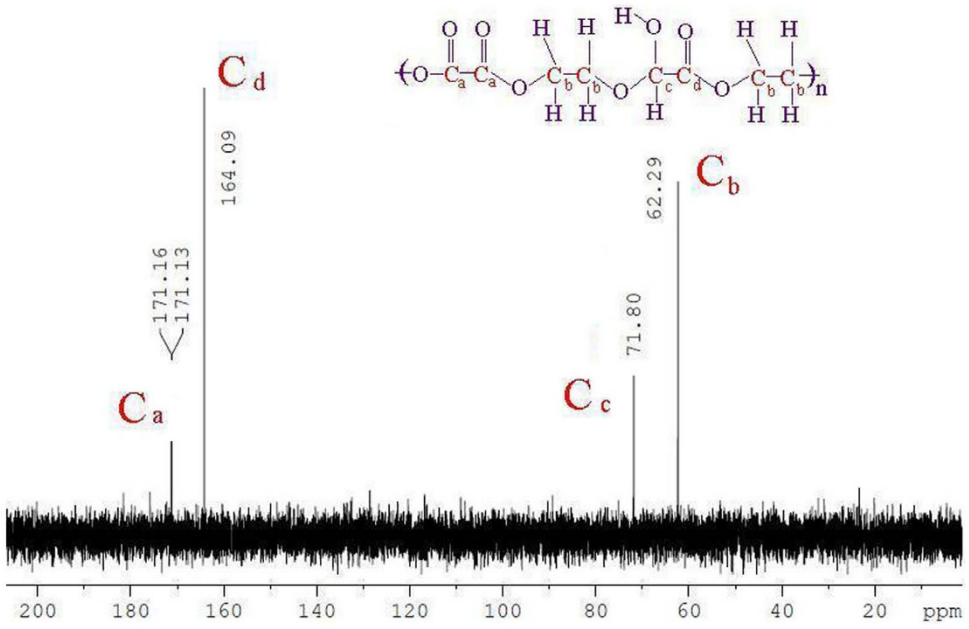

Figure 4 | The ^{13}C NMR results of the polymer. It is the ^{13}C NMR spectrum of the polymer. The proposed chemical structure of the polymer is attached in.

$$\text{M-H} + \text{R} \rightarrow \text{M} + \text{R-H} \quad (7)$$

Because oxalate is the main product and the polymer comprise the groups of oxalate, glycol and α-hydroxyl acetic acid. At the same time, CO_2, carbonic acid, high energy hydrogen atom and glyoxal (S. Fig. 7 and 8) exist in the system. The reaction pathways are suggested as Fig. 7.

As shown in Fig. 7, the reaction process should be described as follows:

Firstly, the high energy hydrogen atoms are produced by electrolysis of water[28], and H_2CO_3 (or HCO_3^-) is produced from CO_2.

$$H_2O \rightarrow H^+ + OH^- \quad (8)$$

$$H^+ + M + e^- \rightarrow \text{M-H} \quad (4)(\text{Volmer})$$

$$H_2O + CO_2 \rightarrow H_2CO_3 \quad (9)$$

Secondly, the H_2CO_3 was reduced by the high energy hydrogen atoms, generated oxalate.

$$2\text{M-H} + 2H_2CO_3 \rightarrow H_2C_2O_4 + 2H_2O + 2M \quad (10)$$

Thirdly, the $H_2C_2O_4$ was subsequently reduced by the high energy hydrogen atoms, generated glyoxal. Then the glyoxal reacted with oxalate, (involved in the high energy hydrogen atoms) generated oxalate-glycol polymer.

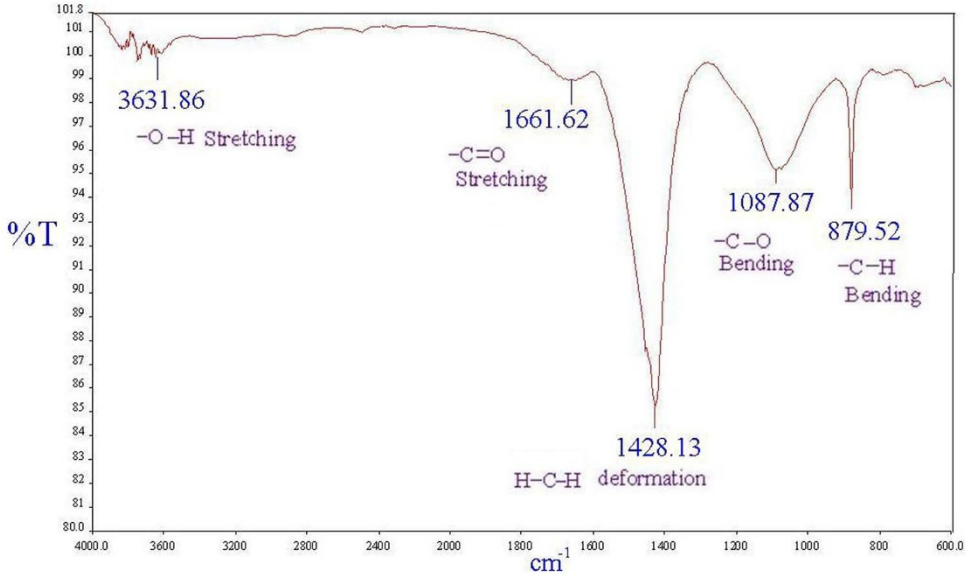

Figure 5 | The FTIR results of the polymer. It is the FTIR spectrum of the polymer. The functional groups of O-H, C=O, C-O, and H-C-H are noted.

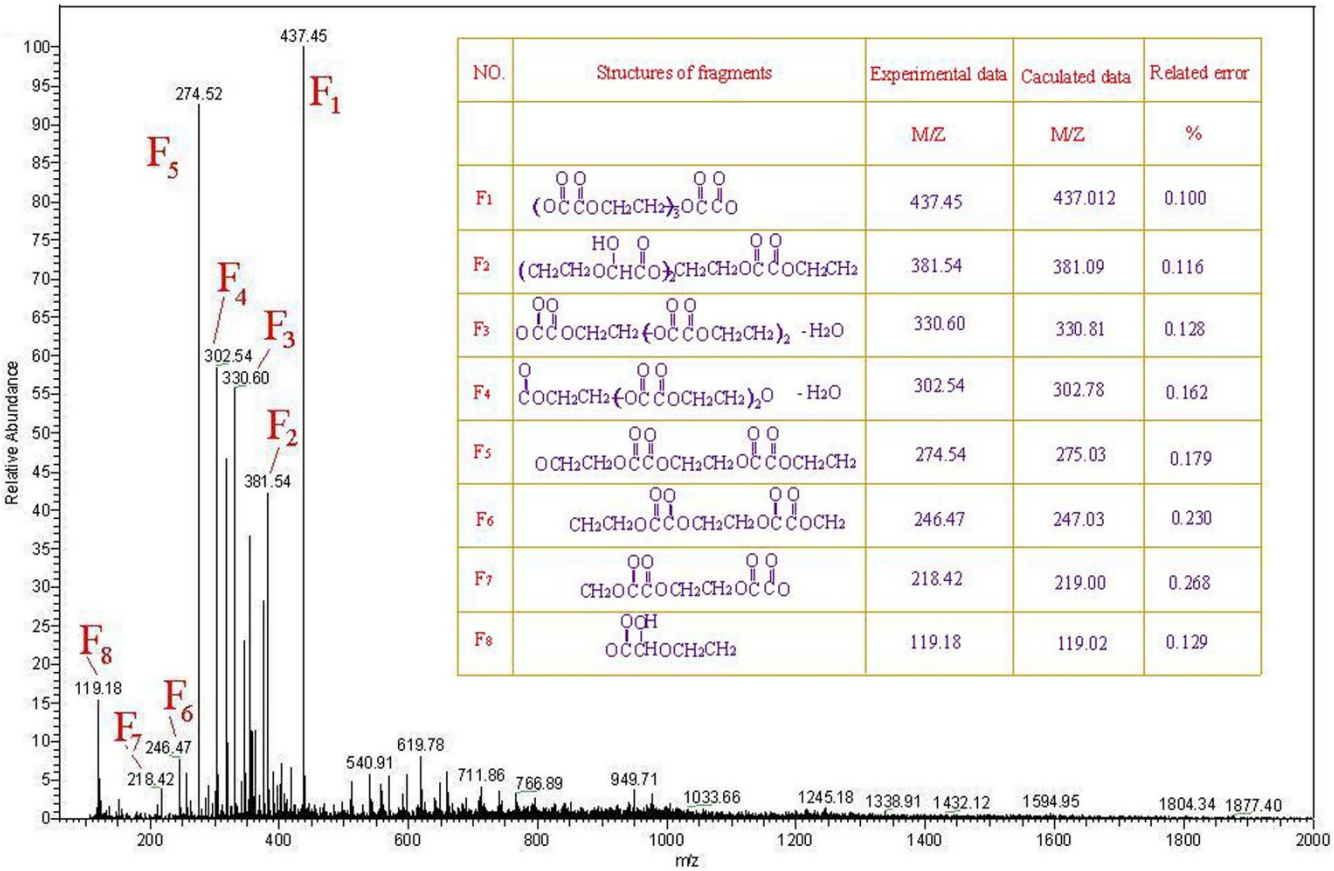

NO.	Structures of fragments	Experimental data	Caculated data	Related error
		M/Z	M/Z	%
F1	$(OCCOCH_2CH_2)_3OCCO$	437.45	437.012	0.100
F2	$(CH_2CH_2OCHCO)_2CH_2CH_2OCCOCH_2CH_2$	381.54	381.09	0.116
F3	$OCCOCH_2CH_2(OCCOCH_2CH_2)_2$ - H_2O	330.60	330.81	0.128
F4	$COCH_2CH_2(OCCOCH_2CH_2)_2O$ - H_2O	302.54	302.78	0.162
F5	$OCH_2CH_2OCCOCH_2CH_2OCCOCH_2CH_2$	274.54	275.03	0.179
F6	$CH_2CH_2OCCOCH_2CH_2OCCOCH_2$	246.47	247.03	0.230
F7	$CH_2OCCOCH_2CH_2OCCO$	218.42	219.00	0.268
F8	$OCHOCH_2CH_2$	119.18	119.02	0.129

Figure 6 | **The MS results of the polymer.** It is the MS spectrum of the polymer. There are eight fragments that were less than 438 m/z, and the structures of the fragments are arrayed in a table attached in the blank of the picture.

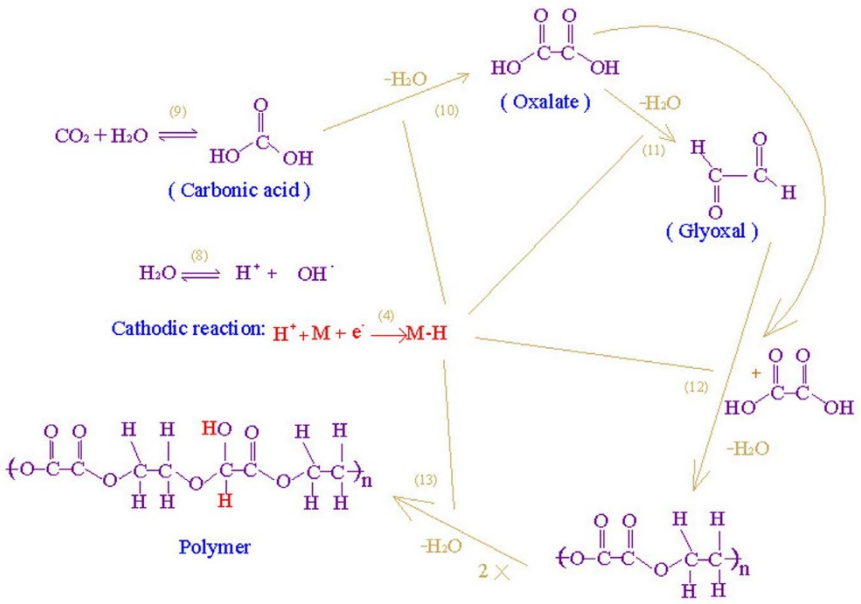

Figure 7 | **The proposed reaction pathways of the artificial photosynthesis.** It is the proposed reaction pathway of the artificial photosynthesis. Four steps of reactions are included.

$$4M\text{-}H + H_2C_2O_4 \rightarrow H_2C_2O_2 + 2H_2O + 4M \quad (11)$$

$$2n\ M\text{-}H + nH_2C_2O_4 + n\ H_2C_2O_2 \rightarrow H(OCOCOOCH_2CH_2)_nOH + (n\text{-}1)\ H_2O + 2n\ M \quad (12)$$

Finally, the oxalate- glycol polymer subsequently was reduced by the high energy hydrogen atoms, generated oxalate-glycol-α-hydroxyl polymer.

$$2nM\text{-}H + 2H(OCOCOOCH_2CH_2)_nOH \rightarrow H(OCOCH(OH)OCH_2CH_2)_nOH + 2nM \quad (13)$$

Methods

Artificial photosynthesis. 600 ml of 5.0%(Wt%)NH_4HCO_3 solution were fed into the electronic cell, its anode and cathode plates were constructed using titanium metal electrode and Nickel-chromium-iron alloy electrode (Ni, 14.2%, Cr, 16.7%, Fe, 69.1%), respectively. A 2.5 μm micro porous membrane of polytetrafluoroethylene (PTFE) was used as the separation membrane. A voltage of 5.0 V was obtained from the accumulator, which was charged from a solar panel with its effective area of 0.25 m^2. The current average 35 mA, the area of cathode plate was 0.00125 m^2. Work at atmospheric condition, room temperature (15–28°C) for 480 hours.

HPLC. The product solution was analyzed by a high performance liquid chromatography, equipped with waters 600 controller and water 2478 dual absorbance detector. The column was a Hypersil C^{18} 5 μm, the temperature of columns was maintained at 50 ± 1°C. The eluent was 0.01 mol/L $(NH_4)H_2PO_4$ solution, added 1.0 mol/L H_3PO_4, PH: 2.7. The flow rate was 1.0 ml/min[29–31].

GPC. 1.00 mg/ml solution of the neutral solid products was prepared and, and it was determined by a gel permeation chromatography (GPC). A HPGPC system equipped with Agilent G1362A differential refraction detector, tree columns of Shodex Sugar KS-801, TSK-G4000PW and KS-G in series were used. The temperature of columns was maintained at 50 ± 1°C, and the eluent was ultra pure water at a flow rate of 1.0 ml/min[32,33].

NMR. ^1H NMR and ^{13}C NMR were carried out on a Spect (600 MHz), using D_2O and TMS as solvent and reference, respectively[34,35].

MS. The polymer was analyzed by a high resolution mass spectrometry (Orbitrap Elite). The polymer was dissolved in methanol and injected at a flow rate of 3 ml/min. The gas temperature was set at 250°C, and the flow rate was 5.0 L/min[36,37].

FTIR. A Fourier Transform Infrared Spectrometer, Speltrum BX, was used. The powdered sample of polymer was on the diamond surface of a special optical tub, and then was analyzed in the range of 7800–350 cm^{-1} [38,39].

HPGC. The evidences for existence of glyoxal are tested by Gas Chromatography (GC). A gas chromatograph (Agilent Technologies 6890N) with a polyethylene glycol column (PEG, INNOWAX) and a flame ionization detector (FID) were used for the analysis[40,41].

Preparation of the standard glyoxal benzene solution: A 5.0 ml of 40% glyoxal water solution was fetched into flash, and dried up at 105°C to obtain the solid glyoxal polymer under the N_2 atmosphere. 20 ml of benzene solvent was added to the flash and heat to 78°C to solve the glyoxal polymer and make the single glyoxal molecular released from the glyoxal polymer. Then the mixture solution was separated by distillation to obtain the fraction containing single glyoxal and benzene solvent, which fraction was used as the standard of single glyoxal benzene solution.

Preparation of the sample of benzene extraction: After reacted for 480 h by artificial photosynthesis, 200 ml produced solution was put in to a flash, and 20 ml benzene solvent was added, then the benzene solvent was obliged to be mix with the produced solution by stirring and shaking to extract single glyoxal. After let stand for 10 minutes, the extraction of benzene solvent was separated from the water solution. That extraction of benzene solvent was used as the sample to test single glyoxal composition.

1. Sayama, K., Mukasab, K., Abea, R., Abeb, Y. & Arakawa, H. A new photocatalytic water splitting system under visible light irradiation mimicking a Z-scheme mechanism in photosynthesis. *J. Photoch. Photobio. A.* **148**, 71–77 (2002).
2. Arifin, K., Majlan, E. H., Daud, W. R. W. & Kassim, M. B. Bimetallic complexes in artificial photosynthesis for hydrogen production: A review. *Int. J. hydrogen energ.* **37**, 3066–3087 (2012).
3. Lin, J., Ding, Z., Hou, Y. & Wang, X. Ionic Liquid Co-catalyzed Artificial Photosynthesis of CO. *Sci. Rep.* **3**, 1056; DOI: 10.1038/srep01056 (2013).
4. Zhou, H. *et al.* Leaf-architectured 3D Hierarchical Artificial Photosynthetic System of Perovskite Titanates Towards CO_2 Photoreduction Into Hydrocarbon Fuels. *Sci. Rep.* **3**, 1667; DOI: 10.1038/srep01667 (2013).
5. Rosen, B. A. *et al.* Ionic Liquid–Mediated Selective Conversion of CO_2 to CO at Low Overpotentials. *Science.* **334**, 643–644 (2011).
6. Hammarström, L., Sun, L., Å, kermark, B. & Styring, S. A biomimetic approach to artificial photosynthesis: Ru(II)–polypyridine photo-sensitisers linked to tyrosine and manganese electron donors. *Spectrochim. Acta A* **37**, 2145–2160 (2001).
7. Kurayama, F., Matsuyama, T. & Yamamoto, H. A feasibility study of a new photosynthesis bioreactor design using TiO_2 particles combined with enzymes. *Adv. Powder Technol.* **15**, 51–61 (2004).
8. Noorden, R. V. Secrets of artificial leaf revealed. *Nature news* DOI: 10.1038/news.2011.564 (2011).
9. Lee, W., Liao, C., Tsai, M., Huang, C. & Wu, J. C. S. A novel twin reactor for CO_2 photoreduction to mimic artificial photosynthesis. *Appl. Catal. B. Environ.* **132–133**, 445–451 (2013).
10. Kurayama, F., Matsuyama, T. & Yamamoto, H. Kinetic study of a new photosynthesis bioreactor design using TiO_2 particles combined with enzymes. *Adv. Powder Technol* **16**, 517–533 (2005).
11. Ozcan, O., Yukruk, F., Akkaya, E. U. & Uner, D. Dye sensitized artificial photosynthesis in the gas phase over thin and thick TiO_2 films under UV and visible light irradiation. *Appl. Catal. B. Environ.* **71**, 291–297 (2007).
12. Iizuka, K., Wato, T., Miseki, Y., Saito, K. & Kudo, A. Photocatalytic reduction of carbon dioxide over Ag cocatalyst-loaded $ALa_4Ti_4O_{15}$ (A = Ca, Sr, and Ba) using water as a reducing reagent. *J. Am. Chem. Soc.* **133**, 20863–20868 (2011).
13. Wang, B. *et al.* Polymer-drug conjugates for intracellar molecule-targeted photoinduced inactivation of protein and growth inhibition of cancer cells. *Sci. Rep.* **2**, 0766; DOI: 10.1038/srep00766 (2012).
14. Yang, Y. *et al.* Control Self-Assembly of Hydrazide-Based Cyclic Hexamers: In or Out. *Sci. Rep.* **3**, 1059; DOI: 10.1038/srep01059 (2013).
15. Zhou, Y. *et al.* Stable acyclic aliphatic solid enols: synthesis, characterization, X-ray structure analysis and calculations. *Sci. Rep.* **3**, 1058; DOI: 10.1038/srep01058 (2013).
16. Sharma, R. & Bouchard, L. Strongly hyperpolarized gas from parahydrogen by rational design of ligand-capped nanoparticles. *Sci. Rep.* **2**, 0277; DOI: 10.1038/srep00277 (2012).
17. Mao, H., Yu, H., Chen, J. & Liao, X. Biphasic catalysis using amphiphilic polyphenols-chelated noble metals as highly active and selective catalysts. *Sci. Rep.* **3**, 2226; DOI: 10.1038/srep02226 (2013).
18. Dou, D. *et al.* Novel Selective and Irreversible Mosquito Acetylcholinesterase Inhibitors for Controlling Malaria and Other Mosquito-Borne Diseases. *Sci. Rep.* **3**, 1068; DOI: 10.1038/srep01068 (2013).
19. Yang, H., Hu, S., Horii, F., Endo, R. & Hayashi, T. CP/MAS ^{13}C NMR analysis of the structure and hydrogen bonding of melt-crystallized poly (vinyl alcohol) films. *Polymer* **47**, 1995–2000 (2006).
20. Denton, T. T., Hardcastle, K. I., Dowd, M. K. & Kiely, D. E. Characterization of D-glucaric acid using NMR, X-ray crystal structure, and MM^3 molecular modeling analyses. *Carbohyd. Res.* **346**, 2551–2557 (2011).
21. Park, J. G., Kahn, J. N., Tumer, N. E. & Pang, Y. Chemical Structure of Retro-2, a Compound That Protects Cells against Ribosome-Inactivating Proteins. *Sci. Rep.* **2**, 0631; DOI: 10.1038/srep00631 (2012).
22. Zhao, H. *et al.* Green "planting" nanostructured single crystal silver. *Sci. Rep.* **3**, 1511; DOI: 10.1038/srep01511 (2013).
23. Ali, S., Marques, A. V. & Gominho, J. Study of thermochemical treatments of cork in the 150–400°C range using colour analysis and FTIR spectroscopy. *Ind. Crop. Prod.* **38**, 132–138 (2012).
24. Liu, H. Practical spectral analysia for organic compounds [45, 63, 83] (Press of Zheng zhou University, Zheng zhou, 2008).
25. Hoang, C. V., Oyama, M., Saito, O., Aono, M. & Nagao, T. Monitoring the Presence of Ionic Mercury in Environmental Water by Plasmon-Enhanced Infrared Spectroscopy. *Sci. Rep.***3**, 1175; DOI: 10.1038/srep01175 (2013).
26. Dong, Q. Infrared spectrucopy [104, 149] (The Petroleum Chemical industry press, Beijing, 1977).
27. Gardea-Hernández, G. *et al.* Fast wood fiber esterification. I. Reaction with oxalic acid and cetyl alcohol. *Carbohyd. Polym.* **71**, 1–8 (2008).
28. Wu, H. *Electronic chemistry* [86] (Press of chemical industry, Beijing, 2004).
29. Fabrik, I., Čmelík, R. & Bobál'ová, J. Analysis of free oligosaccharides by negative-ion electrospray ion trap tandem mass spectrometry in the presence of $H_2PO_4^-$ anions. *Int. J. Mass Spectrom.* **309**, 88–96 (2012).
30. Haynes, C. A. & De Jesús, V. R. Improved analysis of C^{26}: 0-lysophosphatidylcholine in dried-blood spots via negative ion mode HPLC-ESI-MS/MS for X-linked adrenoleukodystrophy newborn screening. *Clin. Chim. Acta.* **413**, 1217–1221 (2012).
31. Schlummer, M., Brandl, F., Mäurer, A. & van Eldik, R. Analysis of flame retardant additives in polymer fractions of waste of electric and electronic equipment (WEEE) by means of HPLC–UV/MS and GPC–HPLC–UV. *J. Chromatogr. A.* **1064**, 39–51 (2005).
32. Hiller, W. *et al.* On-line coupling of high temperature GPC and ^1H NMR for the analysis of polymers. *J. Magn. Reson.* **183**, 290–302 (2006).
33. Radke, W., Gerber, J. & Wittmann, G. Simulation of GPC-distribution coefficients of linear and star-shaped molecules in spherical pores. 2. Comparison of simulation and experiment. *Polymer* **44**, 519–525 (2003).

34. Strano-Rossi, S. *et al.* Screening for exogenous androgen anabolic steroids in human hair by liquid chromatography/orbitrap-high resolution mass spectrometry. *Anal. Chim. Acta.* **793**, 61–71 (2013).
35. Denisov, E., Damoc, E., Lange, O. & Makarov, A. Orbitrap mass spectrometry with resolving powers above 1,000,000. *Int. J. Mass Spectrom.* **325–327**, 80–85 (2012).
36. Nikcevic, I., Wyrzykiewicz, T. K. & Limbach, P. A. Detecting low-level synthesis impurities in modified phosphorothioate oligonucleotides using liquid chromatography–high resolution mass spectrometry. *Int. J. Mass Spectrom.* **304**, 98–104 (2011).
37. Xu, W. *et al.* Make Caffeine Visible: a Fluorescent Caffeine "Traffic Light" Detector. *Sci. Rep.* **3**, 2255; DOI: 10.1038/srep02255 (2013).
38. Thakur, G., Prashanthi, K. & Thundat, T. Directed self-assembly of proteins into discrete radial patterns. *Sci. Rep.* **3**, 1923; DOI: 10.1038/srep01923 (2013).
39. Kher, A., Udabage, P., McKinnon, I., McNaughton, D. & Augustin, M. A. FTIR investigation of spray-dried milk protein concentrate powders. *Vib. Spectrosc.* **44**, 375–381 (2007).
40. Xiao, L. *et al.* Determination of Gaseous Sulphides in the Black Liquor Pyrolysis Gas. *Asian J. Chem.* **25**, 7247–7250 (2013).
41. Nong, G., Wang, S., Mu, J. & Zhang, X. Kinetics of reaction between dimethyl sulfide and hydrogen in black liquor gasification gas with ZnO catalyst. *Asian J. Chem.* **24**, 3118–3122 (2012).

Acknowledgments

The financial support for this project was from the Guangxi Natural Science Foundation (Grant #: 2013jjFA20001).

Author contributions

G.N. involved in the new ideal and design of the device of artificial photosynthesis. S.W. involved in the preparation of the device of artificial photosynthesis. G.N., S.C., Q.Z., H.M. and S.L. involved in separation, determination and analysis of products. Y.X., P.Z. and W.C. involved in the analysis of mass spectrometry. G.N., S.C. and L.H. prepared the manuscript and all authors reviewed the manuscript.

Additional information

Supplementary information accompanies this paper at http://www.nature.com/scientificreports

Competing financial interests: The authors declare no competing financial interests.

How to cite this article: Nong, G.Z. *et al.* Artificial photosynthesis of oxalate and oxalate-based polymer by a photovoltaic reactor. *Sci. Rep.* **4**, 3572; DOI:10.1038/srep03572 (2014).